PHYSICAL REVIEW LETTERS

Edge-Mediated Dislocation Processes in Multishell Carbon Nano-Onions?

E. Akatyeva,[1] J. Y. Huang,[2] and T. Dumitrică[1,*]

[1]*Department of Mechanical Engineering, University of Minnesota, Minneapolis, Minnesota 55455, USA*
[2]*Sandia National Laboratories, Albuquerque, New Mexico 87185, USA*
(Received 8 May 2010; published 1 September 2010)

We report *in situ* electron microscopy observations of dislocation dissociation and annihilation processes in individual nanometer-sized carbon onions. Essential for these processes is the counter-intuitive motion of the $\frac{1}{2}\langle 0001 \rangle$ edge from the outer surface to the inner region, which cross-links or unlinks a large number of shells. The correlation with atomistic simulations and analysis of the energy which separates the strain and edge components indicates that this inward glide originates in the reduction of edge with each inwards glide step, an effect specific to the spherical topology.

Graphite has long served as a model material to understand dislocations. An early work on natural graphite provided factual evidence for the existence of screw dislocations [1]. Recently, synthetic carbon nanostructures began to be explored [2,3] in order to understand dislocations at the nanoscale. Here we study the $\frac{1}{2}\langle 0001 \rangle$ edge dislocation [4] in nested multishell carbon onions [5,6], a complex system that was not considered before. The differences with respect to the planar case transpire from Fig. 1, presenting the screw dipole of the *AA* graphite [7] accommodated in an icosahedral nano-onion. In the planar case, Fig. 1(a), the dislocation loop contains two parallel screws [light gray (green)], which link neighboring shells through deformed sp^2 bonds, and two unpaired [dark gray (red)] parallel armchair edges of the same size. In the spherical case, Fig. 1(b), the screw components are directed radially. The two edges left unpaired [dark gray (red)] in the outermost and innermost shells not only have different curvatures but also show a significant disparity in length. All shells are cross-linked and an Archimedean spiral can be traced between the two edges.

We report that carbon onions exhibit dislocation dynamics very different from those of the crystalline bulk phase and even carbon nanotubes. The asymmetry introduced by the spherical topology reflects in an unexpected attraction of dislocations towards the core, as abundantly observed experimentally in dislocation dissociation and annihilation processes. Microscopic calculations carried out on idealized onions combined with rigorous energy analysis reveal a robust inward driving force on the outer $\frac{1}{2}\langle 0001 \rangle$ edge associated with a reduction in the number of dangling bonds. This force, intrinsic to the spherical topology, is able to account for the experimental observations. The provided microscopic modeling is the first attempt to describe and rationalize dislocation processes in nano-onions.

Our experiments were conducted inside a high resolution transmission electron microscope attached to a Nanofactory STM. Carbon nano-onions coexist with nanotubes produced by arc discharge, with the onions being attached to the surface of the tubes. The STM probe inside this platform was manipulated to contact individual nanotubes, Fig. S1 in the supplementary material [8], but not nano-onions. We pass a high current to Joule heat these nanostructures to a temperature close to 2000 °C [9]. At such a high temperature and under electron radiation, pre-existing dislocations in nano-onions become highly mobile, without the application of any mechanical forces [8].

Figure 2 illustrates the observed interactions of two non-radially aligned $\frac{1}{2}\langle 0001 \rangle$ and $\frac{1}{2}\langle 000\bar{1} \rangle$ edges located three shells under the surface of a nearly spherical onion. Although immediately next to each other, due to the large azimuthal distance the two edges cannot recombine. Instead they dissociate in a sequential way, with the lower edge migrating radially inwards, crossing eight shells, Fig. 2(b), and eventually vanishing into the core, Fig. 2(c). Note that this intriguing inwards glide phenomenon was not observed in multiwalled carbon nanotubes [2,3]. During the same
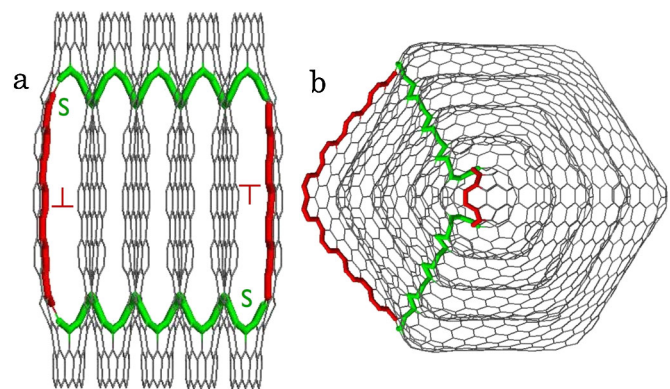

FIG. 1 (color online). (a) A screw dipole in *AA* graphite corresponds to (b) a 3D spiroid [18] in a carbon nano-onion. The latter structure was derived from of a $C_{60}@\ldots$ $@C_{60n^2}@\ldots@C_{1500}$ sequence of five icosahedral fullerenes. The length of the free edge [dark gray (red)] is twice the length of the icosahedral edge. The inner (outer) edge contains four (sixteen) undercoordinated atoms.
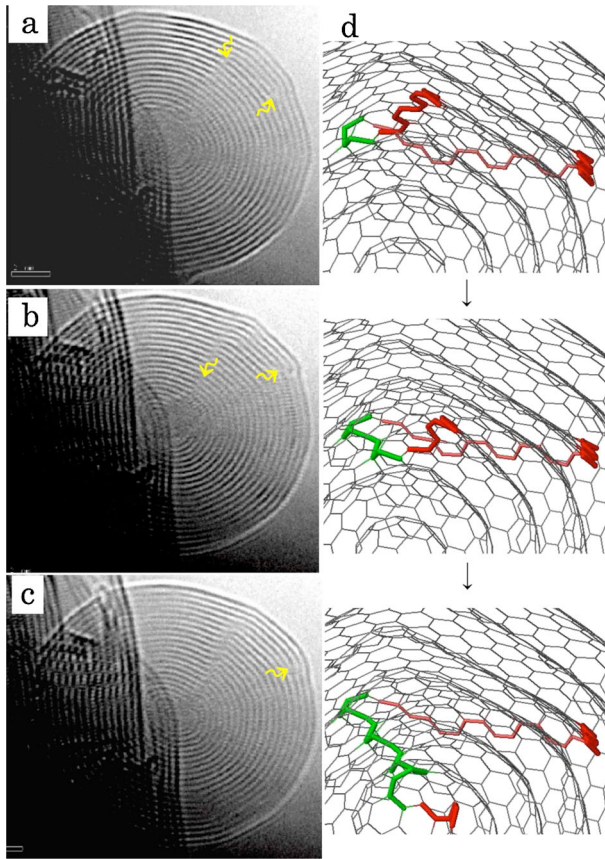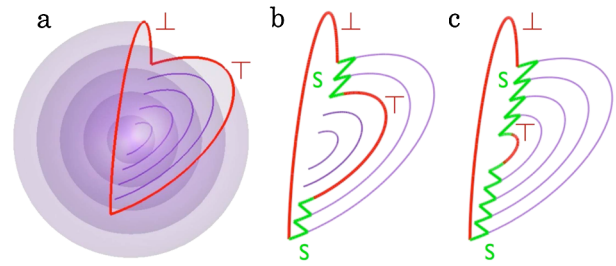
FIG. 3 (color online).   Proposed mechanism for the creation of
a screw dipole in a nano-onion exposed to high temperature and
electron irradiation. (a) The outermost shell breaks, creating a
void with two edges [thicker dark gray (red) line]. (b),(c) The
right edge glides inwards, cross-linking the shells left behind. A
dislocation loop composed of two edge and two screw compo-
nents is formed. For clarity, only the dislocation loop and the
gliding edge former or future position are shown.

Turning back to experiment, Fig. 4 shows the opposite
process of dislocation annihilation. Under prolonged
electron radiation, nano-onions are known to behave as
self-compressed high-pressure cells [10], to the extent that
the large pressure buildup within the cores can lead to the

FIG. 2 (color online).   (a)–(c) *In situ* observation of dislocation
dissociation in a nano-onion of ∼10 nm in radius. Arrows point
out the dislocation edges. (d) An atomic structural model for the
inwards glide of the lower edge with cross-linking of the shells.
The atoms in dark gray (red) [light gray (green)] belong to the
edge [screw] component of the dislocation loop.

time span the upper edge exhibits a contrasting slow
mobility in the outward direction. As shown in Fig. 2(c),
this edge is visible under the two outermost shells.
Figure 2(d) provides microscopic insight into the disloca-
tion dissociation process. It is important to realize that the
two edges are initially connected by two screw dislocations
(only one is visible in the shown cross sections), which link
the two shells. Next, the inwards migration of the lower
edge occurs with cross-linking of the shells.

In several nano-onions we observed isolated $\frac{1}{2}\langle 0001 \rangle$
edges on the outermost shell. Based on the observed
dislocations dissociation, we propose in Fig. 3 a logical
explanation for the presence of such edges: The evapora-
tion of carbon atoms leads to localized breakage of the
outermost shell and creation of a void exhibiting two edges
of opposite sign, $\frac{1}{2}\langle 000\bar{1} \rangle$ and $\frac{1}{2}\langle 0001 \rangle$. Because of the large
azimuthal separation, these edges cannot recombine.
Instead one edge may undergo an inwards glide accompa-
nied by cross-linking of the shells left behind. This way, a
3D spiroid is created, which is characterized by a disloca-
tion loop composed of two edges residing near the inner-
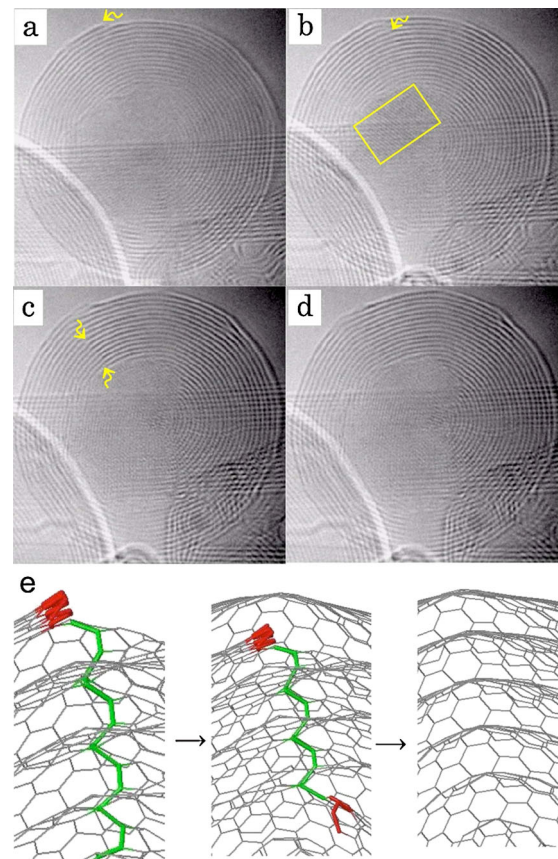most and on the outermost shell.

FIG. 4 (color online).   (a)–(d) *In situ* observation of dislocation
annihilation. Arrows point out the dislocation edge. In (b), a
cubic-diamond region is visible in the highlighted rectangle.
(e) An atomic structural model of the annihilation process
accompanied by unlinking of the shells. The atoms in dark
gray (red) [light gray (green)] belong to the edge [screw]
component of the dislocation loop.

nucleation of cubic-diamond crystals [9,11]. Such a transformation is observed here, Fig. 4(b), signaling that the inhomogeneous pressure build is significant for the present experimental conditions. An edge dislocation with a Burgers vector of $\frac{1}{2}\langle 0001 \rangle$ is visible on the outermost shell, Fig. 4(a). This edge undergoes an inwards glide, in spite of the high pressure at the core: The edge is shown after crossing two, Fig. 4(b), and six outer shells, Fig. 4(c). A second edge dislocation of $\frac{1}{2}\langle 000\bar{1} \rangle$ emerges slowly from the core, Fig. 4(c). The two edges recombine fast in the neighborhood of the core, as the azimuthal separation is smaller. Nearly spherical concentric shells can be noted in the last sequence of Fig. 4(d). Based on the model shown in Fig. 3, it is now easy to see the underlying microscopic path for this process: the nano-onion contains a dislocation loop consisting of one inner and one outer edge and two radial screw components linking the shells located in between. The inward glide of the outer edge unlinks the shells left behind, Fig. 4(e).

Essential to the observed dissociation and annihilation processes is the vigorous inwards motion of an edge located on or near the outermost shell. It is important to recall that in our experimental conditions shells may lose carbon atoms, especially at the edges. Atom migration between shells might occur [12]. However, due to the stochastic nature, these aspects might not play a main role in the coherent inwards glide. It is also worth noting that the known effect of inhomogeneous pressure build up makes the motion towards the higher pressure inner region unexpected. Our observations are also against the known effect of the attraction of dislocations by free surfaces [3]. What else, besides cross-linking and unlinking of shells, goes on in the course of the inwards glide?

In order to address this question, we carried out microscopic calculations based on a modified Brenner's bond-order potential [13]. Although not a genuine representation of the nano-onions encountered in experiment, a 3D idealized spiroid derived from a nano-onion with icosahedral equispaced shells can give significant insights. An icosahedral fullerene is composed of 20 identical equilateral triangles of graphene disposed such that their corners form 12 five-membered rings. In the most stable onion structure, the triangular surfaces in different shells lie directly above one another in a AA-like stacking. The five-shell model spiroid shown in Fig. 1(b) was generated by cutting each shell along like edges. In each shell, the two created armchair edges undergo slipping across each other in the radial direction by an amount equal to the interlayer spacing. Note that each edge (except C_{60}) contains $2(n-1)$ dangling bonds per triangular site and thus neighboring edges (containing two triangular sites) differ by four dangling bonds. Although of different size, the triangle edges of the neighboring shells will fit together seamlessly (without dangling bonds) through sp^2 bonding and sp^3 bonding at the corners. Because of the van der Waals forces there is still equal spacing, $h = 3.4$ Å, between shells.

To probe the dislocation dynamics we studied the detailed energetics of the sequential spiroid-to-onion transformation. Because the spiroid is less energetically favorable, the transformation to the optimal onion form is likely. There are two ways in which this transformation may occur: starting from the innermost shell and gliding outward, and the other way around. Figure 5(a) shows the configurations of the first glide sequence for each route, while Fig. 5(b) plots the calculated energies for the full spiroid-to-onion transformation. As suggested by experiment, an intermediate sp^3 linking state between the stages was considered as the edge passes each shell. Interestingly, we obtain that the two routes are nonequivalent and only the inwards glide of the upper edge is energetically downhill. Hence, this route should dominate the dynamics, as also seen in experiment.
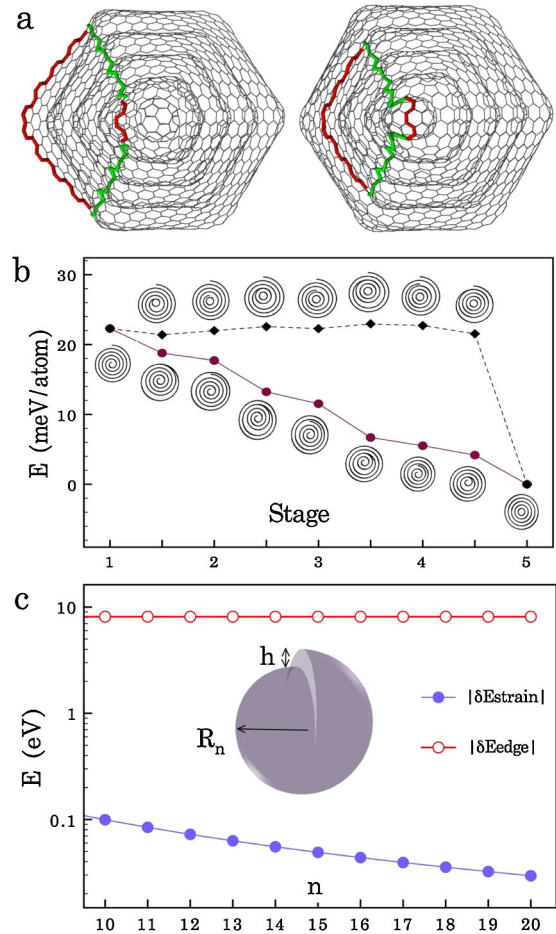

FIG. 5 (color online).   (a) Configuration of the second stage for the two considered routes: inside-to-outside (left-hand side) and outside-to-inside (right-hand side). (b) Energetics of the transformation at each stage: inside-to-outside (filled squares) and outside-to-inside (filled circles). A schematic of the cross section is shown at each point. (c) $|\delta E_{\text{edge}}|$ and $|\delta E_{\text{strain}}|$ in large radius C_{60n^2} shells, as extrapolated from the microscopic data. n is the shell index and δE_{strain} is the difference in strain energy between a spherical and spiroid shell (inset) of same radius R_n.

It is useful next to elaborate on the energy between two consecutive stages, i and $i + 1$,

$$E_{i+1} - E_i = \delta E_{\text{edge}} + \delta E_{\text{strain}}. \qquad (1)$$

Here, the difference in van der Waals energy has been neglected. δE_{edge} captures the change in edge energy, which is stage independent for the ideal case studied here. Most importantly, it should be noted that δE_{edge} has a negative value only in the outside-to-inside route. The release of strain energy, δE_{strain}, is stage dependent and negative for both routes. In the outside-to-inside route, δE_{edge} and δE_{strain} are negative and both contribute to the inwards glide. By contrast, the outwards glide is driven only by the release of strain. Figure 5(b) indicates that the lowering in strain energy is countered by the increase in edge energy. Thus, although possible, no efficient outwards glide is expected in the nano-onion's core.

Gaining insight into larger systems is possible by relating the individual bond strain with the gross elastic deformation. We first approximate δE_{strain} with the difference in strain energy of the specific shell that undergoes the spiroid-to-onion change at a given stage. Next, we account for the microscopic strain in the icosahedral shell viewed as the union of 12 truncated cones (pentagonal disclinations of 60°). The strain energy of one cone comprises both bending energy of the sheet and local effects [14]. It is given by $E_{C_{60}} + (11\pi/5)D \ln n^2$, where $E_{C_{60}}$ is the total excess energy of C_{60}, and D is a bending rigidity of graphene. Finally, we make the spherical shell approximation and equate this energy with $4\pi D_n^{\text{eff}}(1 + \nu)$, where $\nu = 0.165$ is the Poisson ratio for graphene. This way a continuum shell with a size-dependent effective rigidity D_n^{eff} is defined. Relying on this shell model and on the standard procedures of linear elasticity [15] applied to a 3D spiroid shell [16] of mean radius R_n, we obtained

$$|\delta E_{\text{strain}}| = 1.7 D_n^{\text{eff}}(h^2/R_n^2) + O(h^4/R_n^4). \qquad (2)$$

Using an edge energy of 2.0 eV/atom, fitting to our atomistic data of Fig. 5(b) gives $D = 1.67$ eV, in good agreement with the actual value. With this parametrization, Eqs. (1) and (2) provide a reliable basis for comparing the two routes outside the core region. Using it, we predict that for larger diameter shells, as those encountered in experiment, $|\delta E_{\text{strain}}|$ is negligible in comparison with $|\delta E_{\text{edge}}|$, Fig. 5(c). Thus, the outwards glide should be very unlikely outside the core region. Because of the consistent edge lowering effect, the inwards glide appears viable for processes involving both cross-linking, such as dislocations dissociation, and unlinking, such as dislocations annihilation.

Dislocation processes have important implications, especially for mechanical properties. Because of their spherical shape, nano-onions are researched for tribological applications [17]. The efficient cross-linking achieved by dislocation glide may prevent shell sliding, thus modifying the friction-reducing properties. The transport of carbon atoms in graphitic lattices is of great importance, and the ability of carbon atoms to jump between the graphitic shells has been already recognized [12]. An inwards glide appears an easier route to transport atoms through the dislocation line and could shed light on the growth mechanism of nano-onions. Ozawa et al. [18] proposed spiroidal growth, in which all shells become first cross-linked through an onion-to-spiroid interchange. The spiroid stage favors accretion of carbon atoms on the outside edge. In light of our results, a postgrowth retrieving of the nested onion via an inwards glide appears very likely.

*Corresponding author.
td@me.umn.edu.
[1] F. H. Horn, Nature (London) **170**, 581 (1952).
[2] J. Y. Huang, F. Ding, K. Jiao, and B. I. Yakobson, Small **3**, 1735 (2007).
[3] J. Y. Huang, F. Ding, and B. I. Yakobson, Phys. Rev. Lett. **100**, 035503 (2008).
[4] B. T. Kelly, *The Physics of Graphite* (Applied Science, London, 1980).
[5] H. W. Kroto and K. McKay, Nature (London) **331**, 328 (1988).
[6] D. Ugarte, Carbon **33**, 989 (1995).
[7] I. S.-Martinez, G. Savini, G. Haffenden, J.-M. Campanera, and M. I. Heggie, Phys. Status Solidi C **4**, 2958 (2007).
[8] See supplementary material at http://link.aps.org/supplemental/10.1103/PhysRevLett.105.106102 for supporting material.
[9] J. Y. Huang, Nano Lett. **7**, 2335 (2007).
[10] L. Sun, A. V. Krasheninnikov, T. Ahlgren, K. Nordlund, and F. Banhart, Phys. Rev. Lett. **101**, 156101 (2008).
[11] F. Banhart and P. M. Ajayan, Nature (London) **382**, 433 (1996).
[12] Y. Gan and F. Banhart, Adv. Mater. **20**, 4751 (2008).
[13] D. W. Brenner, Phys. Rev. B **42**, 9458 (1990).
[14] J. Tersoff, Phys. Rev. B **46**, 15 546 (1992); A. Siber, Nanotechnology **17**, 3598 (2006).
[15] L. D. Landau and E. M. Lifshitz, *Theory of Elasticity* (Pergamon, Oxford, 1986).
[16] In cylindrical coordinates (θ, z), this spheroid is described by $\rho = [h(\theta/2\pi - 0.5) + R_n]\sqrt{1 - z^2/R_n^2}$.
[17] R. Tenne, Nature Nanotech. **1**, 103 (2006).
[18] M. Ozawa, H. Goto, M. Kusunoki, and E. Osawa, J. Phys. Chem. B **106**, 7135 (2002).